

# Visual Pre-training for Navigation: What Can We Learn from Noise?

Yanwei Wang  
MIT CSAIL  
yanwei@mit.edu

Ching-Yun Ko  
MIT RLE  
cyko@mit.edu

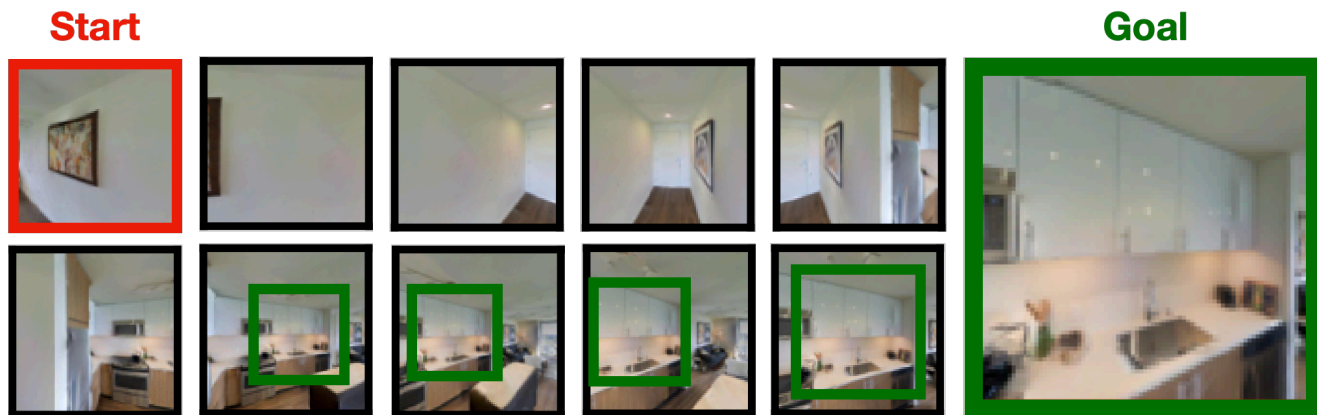


Figure 1: Inference rollout of our navigation policy pre-trained with random crop prediction on noise images. Given a goal view and the current view, the agent first explore the environment by panning its camera. Once the goal view is detected, shown by the green bounding box, the agent moves towards the goal to complete the task. **Click the image for a video.**

## Abstract

A powerful paradigm for sensorimotor control is to predict actions from observations directly. Training such an end-to-end system allows representations that are useful for the downstream tasks to emerge automatically. In visual navigation, an agent can learn to navigate without any manual designs by correlating how its views change with the actions being taken. However, the lack of inductive bias makes this system data-inefficient and impractical in scenarios like search and rescue, where interacting with the environment to collect data is costly. We hypothesize a sufficient representation of the current view and the goal view for a navigation policy can be learned by predicting the location and size of a crop of the current view that corresponds to the goal. We further show that training such random crop prediction in a self-supervised fashion purely on random noise images transfers well to natural home images. The learned representation can then be bootstrapped to learn a navigation policy efficiently with little interaction data. **Code is available at** <https://github.com/yanweiw/noise2ptz>.

## 1. Introduction

Consider how a newborn baby learns to walk. Initially, the baby still lacks motor skills to move around. Nevertheless, she can actively move her eyes around to collect abundant visual data, with which she can potentially learn a predictive model that predicts how she should move her eyes from one view to the next view. The predicted eye movements can thus be a useful representation for navigation, and can be bootstrapped to learn walking from one view to the next view in a few shots once she acquires the locomotive capability. Similarly, in the case of visual navigation, an intelligent agent should first learn how to move its sensor around to find a promising direction to explore before executing any locomotive actions. Concretely, given a current image and a goal image, the agent should encode them into a meaningful state representation that makes the downstream motor policy easy to learn.

But what is the right feature space for predicting a navigation command? A potentially useful representation can be the relative 2D transformation between two views. If we can locate a goal image as a crop centered inside the current field of view, the agent should move forward to get closer. If the crop is to the right of the current field of view, the

agent should then turn right, and vice versa. The relative 2D location of the two views can thus be parametrized by the location and size of a crop of one view that corresponds to the other view. This parametrization is analogous to PTZ factors a camera uses to pan, tilt and zoom onto the current view in order to focus on the goal part. Such a PTZ vector encodes the relative spatial transformation between two views, and can be used to learn a downstream navigation policy. Since the PTZ encoding is low-dimensional compared to the pixel representation of two views, learning a navigation policy from PTZ should require far less robot interaction data than learning directly from pixel inputs. Additionally, an embedding space learned directly from pixels is likely to suffer from distribution shift as we move from training images to testing images, thus adversely affecting the downstream policy’s accuracy. On the contrary, a robot policy that inputs the PTZ parametrization, which only captures relative transformation, will be insulated from the visual statistics changes as we shift from one image domain to the other.

The goal of this project is to test the hypothesis that a pre-trained PTZ predictor can lead to efficient learning of a navigation policy with few robot interaction data in a never-before-seen environment. Crucially, we train the PTZ module by predicting random crops of training environment images in a self-supervised fashion, thus the data involved does not count towards robot interaction data. Our major contribution is that we show training on random noise images can also produce a sufficiently performing PTZ encoder for downstream navigation tasks even in photo-realistic testing environments.

## 2. Related Works

Self-supervision has recently emerged as one of the most promising approaches to ease the need for supervision and yet maintain high performance. Self-supervision builds on the fact pretext tasks can be very useful for pre-training networks without the need for expensive manual annotations. With such pre-trained networks, only a modest amount of labelled data will be needed to fine tune for a target task.

As early as 1981, authors of [13] have made attempts to reduce the reliance on abundant image pair comparisons in image registration by using spatial intensity gradient information as guidance to direct the search for the position that yields the best match. By taking more information about the images into account, the technique is able to find the best match between two images with far fewer comparisons of images. Similarly, the early work of [5] on perceptual learning replaced the external teacher by internally derived teaching signals that are generated based on the assumption that different parts of the perceptual input have common causes in the external world. Specifically, modules that look at different modalities such as vision and

touch, or the same modality at different times such as consecutive 2D views of a rotating 3D object, or spatially adjacent parts of the same images, tend to produce outputs that agree with each other. These resources efficient learning methods have also been exploited in the recent decade [1, 6, 9, 11, 12, 14, 16, 19, 20, 24, 25, 29, 15, 18, 3, 8] with the popularity of deep learning.

Among them, authors of [1] exploit information about egomotion (camera motion), which, unlike the knowledge of class labels, is freely available to mobile agents. With the same number of training images, features learned using egomotion as supervision compare favourably to features learned using class-label as supervision on the tasks of scene recognition, object recognition, visual odometry and keypoint matching. In [2], the robot gathered over 400 hours of experience by executing more than 100K pokes on different objects to learn intuitive model of physics, which is shown effective for planning actions in real-world robotic manipulation tasks. In [22], authors aim to learn to predict grasp locations via trial and error. Different from its earlier literature, authors present a staged-curriculum based learning algorithm, where they learn how to grasp and use the most recently learned model to collect more data. Furthermore, agents in [21] explore the environment without any expert supervision and distills this exploration data into goal-directed skills, as opposed to accounting experts for providing multiple demonstrations of tasks at training time in the form of observation-action pairs from the agent’s point of view.

Interestingly, some pretext tasks are argued to be useful for feature learning in general. For example, [28] shows that colorization can be a powerful pretext task as it serves as a cross-channel encoder. Deep features (e.g. ImageNet-trained VGG features) are also demonstrated to be remarkably useful as a training loss for tasks including image synthesis and outperform all previous metrics by large margins in [30]. In [26], it is found out that pre-training on vision tasks (e.g. object detection) significantly improves generalization and sample efficiency for learning to manipulate objects. Therefore, directly transferring model parameters from vision networks to affordance prediction networks can result in successful zero-shot adaptation, where a robot can pick up certain objects with zero robotic experience. A comprehensive study [27] is proposed recently giving analysis of self-supervision. Specially, authors conclude that the weights of the early layers in a deep network contain low-level statistics of natural images, which can be learned decently through solely self-supervision or captured via synthetic transformations instead of using a large image dataset.

Slightly more related are works that exploit the possibility of pre-training without natural images [10, 17]. Recently, authors of [10] generate image patterns and their cat-

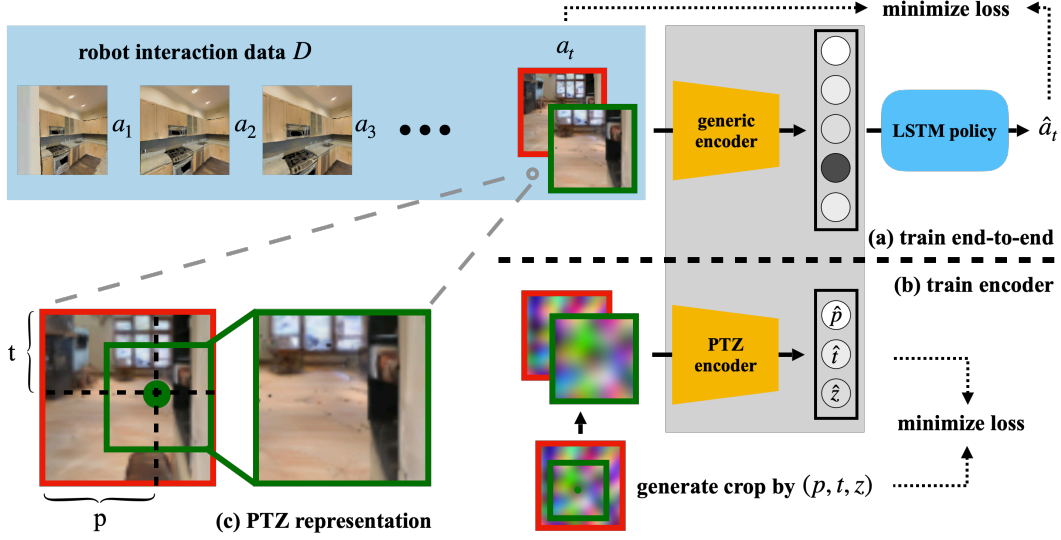


Figure 2: The visual navigation frameworks. Top (a): an end-to-end training baseline, where a generic feature space is jointly learned by minimizing cross entropy loss between  $a_t$  and  $\hat{a}_t$  for all image-action sequences in  $D$ . Bottom: (b) a proposed encoder pre-training, where we assume (c) the goal view can be seen as a crop from the current view and use the relative panning, tilting and zooming factors (PTZ) between two (synthetic, e.g. random noises) image crops to perform the pre-training.

egory labels to construct FractalDB, a database without natural images, automatically by assigning fractals based on a natural law existing in the background knowledge of the real world. [17] further demonstrates the usefulness of FractalDB in pre-training Vision Transformers (ViTs). Beyond fractal noise, [4] provides a comprehensive study on how different noise types affect representation learning.

### 3. Method

Given a robot interaction dataset  $D$ , we want an agent to navigate to a goal location upon receiving a goal image  $x_g$ . The dataset  $D$  consists of image action pairs  $(x_t, a_t, x_{t+1})$ , where  $x_t$  is the pixel observation at time  $t$ ,  $a_t$  the action taken at time  $t$ , and  $x_{t+1}$  the pixel observation after the action. One approach to learn a navigation policy is to train an inverse model on  $D$ , which predicts an action given a current view and a goal view [2]. As memory of past states and actions benefits navigation with only partial observations [21], we divide the inverse model into an encoder  $E_\phi$  that encode image pairs into states and an LSTM policy  $\pi_\theta$  that predicts actions conditioned on states as in Eq (1)

$$\hat{s}_t = E_\phi(x_t, x_{t+1}) \quad \hat{a}_t = \pi_\theta(\hat{s}_t). \quad (1)$$

We can train  $E_\phi$  and  $\pi_\theta$  jointly end-to-end by minimizing cross entropy loss between  $a_t$  and  $\hat{a}_t$  for all image-action sequences in  $D$  as shown in the top part of Fig 2 (a).

The benefit of such an approach is that the system can automatically find the right parameters for a generic encoder such that the learned state representation  $s_t$  is useful for the downstream policy. The lack of inductive bias, however, requires a lot of interaction data to train the whole pipeline, which can be expensive to collect. While using interaction data to supervise the navigation policy  $\pi_\theta$  is fair, using it to train also a generic feature encoder  $E_\phi$  seems wasteful. Specifically, the encoding of an image pair should not depend on the action space, and it should work even when the two images are not associated with a particular action. Additionally, the fact that in navigation the action space is typically low dimensional also means most data will be used to learn a mapping from high-dimensional pixels to low dimensional states rather than from states to actions. To focus interaction data on learning the policy  $\pi_\theta$ , we can introduce a pre-trained encoder as a fixed feature extractor to replace the generic encoder.

To find out what information the feature encoder should encode, we observe in Fig 2 (c) that a goal view can be seen as a crop from the current view. The relative location and size of the crop indicates the relative heading and distance of the agent from the goal location. Thus the relative transformation between the two views can be parametrized by the panning angle  $p$ , tilting angle  $t$ , and zooming factor  $z$ , which a PTZ camera can use to shifts its current field of view to a goal field of view. We hypothesize such a 3 DOF parametrization is sufficient for local navigation where a



Figure 3: Examples of the random crop generation process, where the black boxes are the original images, the red boxes are generated current view, and the green boxes are generated goal view.

goal is close to the agent. The low dimensionality of this action space is desirable as the mapping between states and actions can be learned efficiently with a few data points. We will now discuss our implementation of the PTZ encoder that predicts  $(p, t, z)$  given two images.

**PTZ Encoder** Similar to how digital PTZ is implemented by cropping the current view to generate the panned, tilted, and zoomed view, we approximate learning a PTZ encoder with learning a random crop predictor. Given an  $256 \times 256$  image, we randomly crop a  $128 \times 128$  pixel patch to form the current view. For the goal view, we randomly sample a scale factor  $z$  from  $0.5 - 1$  and  $(p, t)$  from  $0 - 1$  relative to the top left corner of the first crop to generate the second crop at the location  $(128x, 128y)$ . We resized the second crop to a  $128 \times 128$  pixel patch afterward. Fig 3 visualizes the random crop generation process.

Additionally, we also generate pairs of crops without any overlap. This helps scenarios where the goal view is not directly observable in the current field of view. We assign PTZ label  $(0, 0, 0)$  to such crop pairs corresponding to zero overlap. The ratio between crops that share some overlap and crops that do not overlap at all is 2:1 in our dataset. We will verify later in ablation that including non-overlapping crops prompts the agent to do exploration behavior when it does not see the goal and improves overall navigation performance.

We train a ResNet18 network to regress the PTZ factors  $(p, t, z)$  on concatenated crop pairs from image sources other than the interaction dataset  $\mathcal{D}$  such as standalone natural home images (without action labels) or synthetic images as shown in Fig 2 (b). We replace ResNet18’s fully-connected layer with a linear layer that projects onto a 3-dimensional space followed by a sigmoid activation and use L1 loss for training.

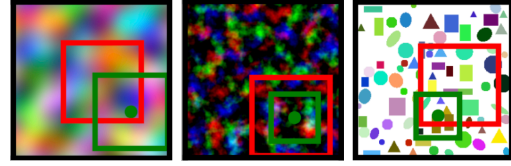


Figure 4: Examples of random noise types. From left to right: Perlin noise, fractal noise, and random geometric shapes.

**Training PTZ Encoding on Random Noise** One potential concern in dividing the whole pipeline into parts and train each part separately is that a well-trained feature encoder from one domain may not transfer well to the navigation task domain. A quick fix is that we can collect data to train the PTZ encoder from the same image domain as the navigation task, i.e. the natural home images. Crucially, this data is not interaction data as the agent does not need to execute any navigation actions to collect. For example, an agent can stand still in the environment and move its sensors around to collect data. An interesting finding as we train the PTZ on natural home images is that the performance transfers well from training domain from testing domain even when we take images from significantly different-looking environments. This suggests learning to predict relative  $2D$  transformations is not tied to the visual statistics of the images on which the learning occurs. We are thus motivated to ask if we can train the PTZ encoder entirely on randomly generated noise images and transfer to natural home images?

To answer this question we first trained our PTZ encoder on Gaussian noise. The resulting poor performance suggests the particular choice of noise is critical. We hypothesize that patterned noise rather than high frequency noise should be more useful as the encoder probably needs some visual cues to find relative transformations. To this end we include Perlin noise, which can be used to simulate cloud formations in the sky, and fractal noise, which can be found in nature [10], in the dataset to train the encoder. We further include random geometric shapes as they are found in man-made environments and can help the encoder learn edges and orientations. A sample of these three different kinds of random noise is shown in Fig 4. We follow the same procedure as before to sample random crops on these noise images. Using noise for pre-training completely removes the need to access an testing environment for data.

**PTZ-enabled Navigation Policy** Given a pre-trained PTZ encoder  $E_\phi$  and the interaction dataset  $\mathcal{D}$ , we can now train the LSTM navigation policy  $\pi_\theta$ . Specifically, we sample sub-trajectories up to a maximum trajectory length from every image-action sequence in  $\mathcal{D}$ . We use  $E_\phi$  as fix feature extractor that encode image pairs into PTZ factors



which become the inputs to  $\pi_\theta$ . Additionally the previous action is also given to the policy following [21]. We use a single layer LSTM network with 512 hidden units with ReLU activation to regress the navigation action with L1 loss. During inference, the LSTM can then be queried with a current view and a goal view at each time step, and predicts an action autoregressively until the agent reaches the goal or the episode terminates. Notice if sub-trajectories of maximum sequence 1 are sampled, the LSTM policy is effectively trained as a feed-forward network that does not use memory from previous time steps.

**End-to-End Baseline Policy** We train the previously described  $E_\phi$  and  $\pi_\theta$  jointly end-to-end by directly predicts  $a_t$  given  $(x_t, x_{t+1})$ . We use ResNet18 as the generic encoding network and modifies a fully connected layer to project onto a 128-dimensional embedding space. The same LSTM then uses the 128-dimensional state plus the previous action to predict the next action. The whole pipeline is trained only with interaction data with cross-entropy loss.

## 4. Experiments

### 4.1. Interaction Data Collection

We use Habitat-Sim as our simulator to render photo-realistic images from 3D apartment models in the Gibson Dataset and a simulated turtlebot as our agent to collect interaction data. The robot action space consists of four actions: stop, move forward by 0.3m, turn left by 20 degrees, and turn right by 20 degrees.

To collect interaction data, the robot explore the environment with the following scheme. The robot is first randomly placed the agent in the environment. The four robot actions are sampled according to probability [5%, 31.67%, 31.67%, 31.67%]. For each sampled action, the agent repeats it uniformly at random 1-2 times if it is ‘stop,’ and uniformly 1-5 times if otherwise. In the event of a collision, the current repeat sequence is aborted, and a turning action is sampled and repeated 5-13 times uniformly at random. Each episode terminates after 50 actions.

For training, we choose ten Gibson environments—‘Crandon,’ ‘Delton,’ ‘Goffs,’ ‘Oyens,’ ‘Placida,’ ‘Roane,’ ‘Springhill,’ ‘Sumas,’ ‘Superior,’ and ‘Woonsocket.’ We create a 20k/10k training/validation set and a 50k/10k training/validation set from sampling 40/20 and 100/20 starting locations in each of the ten environments. We also create a small 1k/1k training/validation set from sampling 20 starting locations from ‘Superior’ and 20 starting locations from ‘Crandon’ respectively. Collectively, we have created three interaction dataset  $D_{2k}$ ,  $D_{30k}$  and  $D_{60k}$ .

### 4.2. PTZ training Data Collection

First, we generate a training set from similar domains to the navigation experiments. Specifically, we sample 6500

photo-realistic home images sourced from 65 Gibson environments rendered by the Habitat-Sim simulator to form the training set and 2300 home images from 23 other Gibson environments to form the test set. Notice these images are generated i.i.d. without any action labels. We refer to this dataset as  $D_{Habitat}$

Second, we generate Perlin noise and fractal noise using [23]. Perlin noise is generated from 2, 4, 8 periods and fractal noise is generated from 2, 4, 8 periods and 1-5 octaves. We generate 10k Perlin noise, 10k fractal noise, and 20k random shapes to form a 40k noise dataset  $D_{noise}$ . However, this particular composition of noise is rather wishful as we do not know yet which one is the best for PTZ encoder training. To uncover which noise is the best surrogate data source for natural home images, we also create a 40k  $D_{Perlin}$ ,  $D_{fractal}$  and  $D_{shape}$ , each containing only one kind of noise.

### 4.3. PTZ Pre-training

We train our PTZ encoder with 5 different data source:  $D_{Habitat}$ ,  $D_{noise}$ ,  $D_{Perlin}$ ,  $D_{fractal}$  and  $D_{shape}$ , and test them with the Habitat natural home image test set and report their results in Tab 1. Although training on  $D_{Habitat}$  converges fast and achieves near perfect testing performance, training on noise images using the same cropping scheme proves slow to convergence. One empirical observation is that non-overlapping crops confuse the encoder when it has not learn to predict PTZ between two overlapping crops well. If we first train the encoder only with overlapping crops to convergence before mixing in non-overlapping crops, we can get high prediction accuracy for both non-overlapping and overlapping crops. We call this indispensable staggered training a curriculum for training with noise. Once we have the pre-trained PTZ encoder  $E_\phi$ , we fix its weights and optimize only the LSTM weights in  $\pi_\theta$  as we train the navigation system with interaction data  $D$ .

### 4.4. Navigation Task

To test our hypothesis that a pre-trained PTZ encoder can improve data efficiency, we consider a local navigation task, where the goal is in the same room as the agent. We choose five environments—‘Beach,’ ‘Eastville,’ ‘Hambleton,’ ‘Hometown,’ and ‘Pettigrew.’ and evaluate our PTZ-enabled navigation policy on multi-step navigation. Specifically, we sample 30 starting and goal locations in each of the testing environments such that the start and the goal are five forward steps apart. We then randomize the heading such that goal be in any direction including behind the agent. Such a design tests not only moving towards the goal when the goal is visible but also exploration capability when the goal is not initially visible. This partial observation of the space prompts the using of an LSTM instead of just a feedforward network as the agent needs to memorize where

Data	Overlap-IOU	Non-Overlap
Shape	$72.1 \pm 0.4\%$	$48.2 \pm 1.1\%$
Perlin	$61.6 \pm 0.4\%$	$65.3 \pm 0.6\%$
Fractal	$87.3 \pm 0.5\%$	$80.1 \pm 0.6\%$
All noise combined	$92.2 \pm 0.1\%$	$93.2 \pm 0.5\%$
Habitat	$97.1 \pm 0.1\%$	$98.8 \pm 0.1\%$
Habitat w/o non-overlap	$96.4 \pm 0.1\%$	$1.5 \pm 0.1\%$
Fractal w/o curriculum	$78.0 \pm 0.4\%$	$2.7 \pm 0.3\%$

Table 1: Performance comparison of PTZ encoders on the 2300 natural home image test set. In the case when the given goal view (partially) overlaps with the current view, we use the IOU between the ground truth box and predicted bounding box of the goal image in the current view as the evaluation metric. In the case when the given goal view does not overlap with the current view, we set the ground truth PTZ label to (0,0,0) and the corresponding success is defined by whether the encoder can give values that are close enough (given a pre-defined tolerance) to (0,0,0). We report the success rates in such non-overlap case.

it has explored when it has yet to find the goal to avoid back-and-forth actions. Since trajectories in  $\mathcal{D}$  are 50 actions long, we also experimented with sampling from them sub-trajectories of different length as inputs to the system. We hypothesize the longer the sub-trajectories we feed into LSTM when training end-to-end, the better testing performance the system will produce as it has seen more variations and developed more nuanced memory of past experience. However, we do not know if this assumption will hold as we introduce the PTZ encoding into the pipeline. We will run inference experiments to clarify these questions.

To infer a trajectory, the agent will auto-regressively predict the next action given the current view and goal view until it uses up to 50 steps or reaches the goal. To determine if an agent arrives at an observation that is close enough to the goal image, we use perceptual loss [30] to measure the similarity between those two observations in the eye of a human. If the similarity score exceeds a threshold of 0.6 while the agent is within a 0.5m radius of the goal location, we consider that agent has successfully reached the target.

## 5. Results

### 5.1. PTZ encoding evaluation

Let us first examine how well our PTZ encoder trained on noise performs on the 2300 natural home image test set. We evaluate our model by calculating the IOU between the ground truth and predicted bounding box of the goal image in the current view when the goal can be at least partially seen (partially overlaps). As the model predicts more accurate PTZ factors, the predicted bounding box will over-

lap with the ground truth bounding box more and IOU will approach 1. If the two images are not overlapping, we report the rate at which the model predicts a state close to the ground truth (0, 0, 0), which corresponds to no detection of goal. For example, if we pre-train the PTZ module with Perlin noise and test with a goal view that does not appear in the current view, then by our definition, the PTZ module should output values close to (0, 0, 0). With a pre-defined tolerance, around  $65.3 \pm 0.6\%$  of non-overlap cases successfully give PTZ values that are close-enough to (0, 0, 0).

In Tab 1, we show mean and standard deviation of inference performance on both overlapping and non-overlapping image pairs of PTZ trained on different data sources. Training on natural home images  $\mathcal{D}_{Habitat}$  naturally produces the highest accuracy. However, we observe that training on all three noises combined  $\mathcal{D}_{noise}$  produces competitive results without seeing a single natural home image. This suggests PTZ of two views is independent of the underlying visual statistics and can transfer well from one domain to another. This property allows for stable training of downstream LSTM policy as PTZ representation will be consistent across different visual domains. This also suggests we do not need to collect new data to fine-tune our navigation policy if we move from one environment to another. We show qualitative inference results of the PTZ encoder in Fig 1 where the green bounding boxes indicate where the PTZ encoder predicts the goal crop in the current view.

To understand which noise is the most helpful for pre-training, we train the PTZ encoder on individual noise  $\mathcal{D}_{Perlin}$ ,  $\mathcal{D}_{fractal}$  and  $\mathcal{D}_{shape}$ . We see in Tab 1 training on fractal noise to convergence outperforms Perlin noise and random shapes and approaches the performance of all noise combined. This result is in line with the finding in [10] and indicates that the natural home images may share more similar visual statistics with fractal noise than others.

The PTZ encoder trained on noise go through a two-stage training curriculum, where we first train with only overlapping images before adding non-overlapping ones. This curriculum is crucial to performance at convergence. If we train on noise images, say  $\mathcal{D}_{fractal}$  with overlapping and non-overlapping crops concurrently from the start, the performance is lower for overlapping IOU and significantly lower for non-overlapping success prediction rate as shown by the results of ‘Fractal w/o curriculum’ in Tab 1. On the one hand, this suggests prediction on overlapping images and non-overlapping images leverage similar features and can enhance the performance of each when trained together in a curriculum. On the other hand, it might be easier to find those features by training on overlapping images alone at first and then bootstrap from those features to learn to recognize images that do not overlap at all later on.

One might ask if non-overlapping images complicate the training, is it necessary to include them? We argue for their

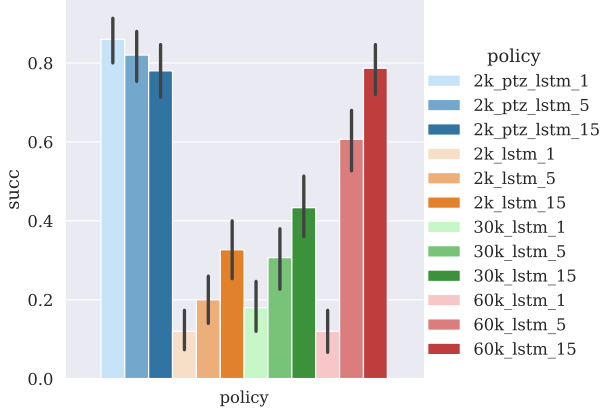


Figure 5: Navigation results comparing data efficiency of PTZ enabled model and training from scratch. With more interaction data being used (60k), the end-to-end training fashion can finally perform decently (approaching 80% success rate), compared to the easily over 80% success rate of our proposal with only 2k interaction data.

necessity as otherwise the prediction on non-overlapping image pairs will be arbitrary and can lead to erroneous inputs to the LSTM policy. We will show in the subsequent section that training the whole system with a PTZ encoder pre-trained on natural home images yet without non-overlap crops gives inferior results.

## 5.2. Navigation policy evaluation

In Fig 5 we show the percentage of successful runs among 30 rollouts for each environment. We compare results from policies trained on interaction data  $D_{2k}$ ,  $D_{30k}$  and  $D_{60k}$ , either with PTZ-enabled LSTM or vanilla LSTM from scratch, and different maximum trajectory length 1, 5 and 15. For a given maximum trajectory length  $n$  we sample sub-trajectories of length  $1-n$  from the collected 50-step image-action sequence. When  $n=1$  we only feed single-action sequences to the LSTM and effectively train it as a feed-forward network without its recurrent memory. We include experiments on feed-forward networks here because [7] reports feed-forward networks are more reactive to state inputs while LSTM tends to blindly mimic the trajectories in the data source. Since the agent collects the interaction data initially through random exploration, the data is highly sub-optimal. We hope including feed-forward network experiments will provide insight into how much the sub-optimality can affect LSTM policies.

We see in Fig 5 that without the PTZ encoding, the success rate of navigating to the goal location increases as we train the whole pipeline with more data. Since the system needs to figure out the right state representation by itself,

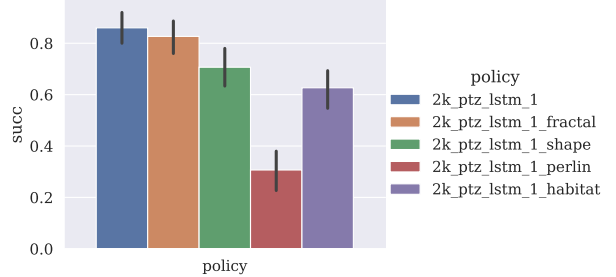


Figure 6: An ablation study. Navigation results comparing the effect of different noises used in pre-training. The performance gap between PTZ encoder trained only with fractal noise (brown bar) and PTZ encoder trained with all noises (blue bar) is marginal, demonstrating the sufficiency of learning a PTZ model only with fractal noise for navigation tasks.

it benefits the learning as we feed longer sequences and introduces more reliance on the behavior demonstrated by the scripted random exploration in the interaction data. However, as we start to introduce PTZ encoding, such support becomes unnecessary. Specifically, training a PTZ-enabled policy with only 2k interaction data, one-action sequence already outperforms training an end-to-end system from scratch with 60k data. As we increase the action sequence length to train the PTZ-enabled system, the performance actually drops. This is potentially due to the fact that the LSTM tries to memorize the action sequence in the interaction data even if it is sub-optimal.

So far we have only demonstrated results on PTZ encoder trained with all three noise. If we use PTZ encoder pre-trained with individual noise source as shown in Tab 1, what will the navigation success rate be? We show in Fig 6 that PTZ encoder trained with fractal noise outperforms Perlin noise and random shapes. Although the evaluation metrics in Tab 1 shows training on fractal noise is inferior to training on all noise combined, the navigation results show that it is sufficient to achieve high success rate for the downstream task using fractal noise for pre-training alone. We also show in Fig 6 that using a PTZ pre-trained without overlapping images ('2k\_ptz\_lstm\_1\_habitat') indeed gives rise to poor navigation policy. Thus, pre-training a PTZ encoder on noise to perform navigation tasks benefits from a curriculum of training first on overlapping crops followed by adding non-overlapping crops.

## 6. Conclusion

In this project, we focus on the topic of visual pre-training for navigation. As training in an end-to-end fashion requires a significant amount of data (60k as shown in Fig-

ure 5), we break the system into two modules: a feature encoder module (PTZ module) and a LSTM policy-making module, where the first part can be effectively pre-trained without the use of expensive interaction data. Three popular noises are included in pre-training the PTZ module and their effectiveness are extensively evaluated. Promising experimental results verify the usefulness of our proposal in reducing the need for interaction data.

## References

- [1] Pulkit Agrawal, João Carreira, and Jitendra Malik. Learning to see by moving. In *2015 IEEE International Conference on Computer Vision (ICCV)*, pages 37–45, 2015. 2
- [2] Pulkit Agrawal, Ashvin Nair, Pieter Abbeel, Jitendra Malik, and Sergey Levine. Learning to poke by poking: experiential learning of intuitive physics. In *Proceedings of the 30th International Conference on Neural Information Processing Systems*, pages 5092–5100, 2016. 2, 3
- [3] Relja Arandjelovic and Andrew Zisserman. Look, listen and learn. In *Proceedings of the IEEE International Conference on Computer Vision*, pages 609–617, 2017. 2
- [4] Manel Baradad Jurjo, Jonas Wulff, Tongzhou Wang, Phillip Isola, and Antonio Torralba. Learning to see by looking at noise. *Advances in Neural Information Processing Systems*, 34:2556–2569, 2021. 3
- [5] Suzanna Becker and Geoffrey E Hinton. Self-organizing neural network that discovers surfaces in random-dot stereograms. *Nature*, 355(6356):161–163, 1992. 2
- [6] Carl Doersch, Abhinav Gupta, and Alexei A. Efros. Unsupervised visual representation learning by context prediction. In *Proceedings of the 2015 IEEE International Conference on Computer Vision (ICCV)*, ICCV ’15, page 1422–1430, USA, 2015. IEEE Computer Society. 2
- [7] Leonard Hasenclever, Fabio Pardo, Raia Hadsell, Nicolas Heess, and Josh Merel. Comic: Complementary task learning & mimicry for reusable skills. In *International Conference on Machine Learning*, pages 4105–4115. PMLR, 2020. 7
- [8] Phillip Isola, Daniel Zoran, Dilip Krishnan, and Edward H Adelson. Learning visual groups from co-occurrences in space and time. *arXiv preprint arXiv:1511.06811*, 2015. 2
- [9] Simon Jenni and Paolo Favaro. Self-supervised feature learning by learning to spot artifacts. In *Proceedings of the IEEE Conference on Computer Vision and Pattern Recognition*, pages 2733–2742, 2018. 2
- [10] Hirokatsu Kataoka, Kazushige Okayasu, Asato Matsumoto, Eisuke Yamagata, Ryosuke Yamada, Nakamasa Inoue, Akio Nakamura, and Yutaka Satoh. Pre-training without natural images. In *Proceedings of the Asian Conference on Computer Vision*, 2020. 2, 4, 6
- [11] Dahun Kim, Donghyeon Cho, Donggeun Yoo, and In So Kweon. Learning image representations by completing damaged jigsaw puzzles. In *2018 IEEE Winter Conference on Applications of Computer Vision (WACV)*, pages 793–802. IEEE, 2018. 2
- [12] Gustav Larsson, Michael Maire, and Gregory Shakhnarovich. Learning representations for automatic colorization. In *European conference on computer vision*, pages 577–593. Springer, 2016. 2
- [13] Bruce D Lucas and Takeo Kanade. An iterative image registration technique with an application to stereo vision. In *Proceedings of the 7th international joint conference on Artificial intelligence-Volume 2*, pages 674–679, 1981. 2
- [14] Aravindh Mahendran, James Thewlis, and Andrea Vedaldi. Cross pixel optical-flow similarity for self-supervised learning. In *Asian Conference on Computer Vision*, pages 99–116. Springer, 2018. 2
- [15] Ishan Misra and Laurens van der Maaten. Self-supervised learning of pretext-invariant representations. In *Proceedings of the IEEE/CVF Conference on Computer Vision and Pattern Recognition*, pages 6707–6717, 2020. 2
- [16] Ishan Misra, C Lawrence Zitnick, and Martial Hebert. Shuffle and learn: unsupervised learning using temporal order verification. In *European Conference on Computer Vision*, pages 527–544. Springer, 2016. 2
- [17] Kodai Nakashima, Hirokatsu Kataoka, Asato Matsumoto, Kenji Iwata, and Nakamasa Inoue. Can vision transformers learn without natural images? *arXiv preprint arXiv:2103.13023*, 2021. 2, 3
- [18] Mehdi Noroozi and Paolo Favaro. Unsupervised learning of visual representations by solving jigsaw puzzles. In *European conference on computer vision*, pages 69–84. Springer, 2016. 2
- [19] Deepak Pathak, Ross Girshick, Piotr Dollár, Trevor Darrell, and Bharath Hariharan. Learning features by watching objects move. In *Proceedings of the IEEE Conference on Computer Vision and Pattern Recognition*, pages 2701–2710, 2017. 2
- [20] Deepak Pathak, Philipp Krahenbuhl, Jeff Donahue, Trevor Darrell, and Alexei A Efros. Context encoders: Feature learning by inpainting. In *Proceedings of the IEEE conference on computer vision and pattern recognition*, pages 2536–2544, 2016. 2
- [21] Deepak Pathak, Parsa Mahmoudieh, Guanghao Luo, Pulkit Agrawal, Dian Chen, Yide Shentu, Evan Shelhamer, Jitendra Malik, Alexei A Efros, and Trevor Darrell. Zero-shot visual imitation. In *Proceedings of the IEEE conference on computer vision and pattern recognition workshops*, pages 2050–2053, 2018. 2, 3, 5
- [22] Lerrel Pinto and Abhinav Gupta. Supersizing self-supervision: Learning to grasp from 50k tries and 700 robot hours. In *2016 IEEE international conference on robotics and automation (ICRA)*, pages 3406–3413. IEEE, 2016. 2
- [23] Pierre Vigier. perlin-numpy. <https://github.com/pvigier/perlin-numpy>, 2018. 5
- [24] Xiaolong Wang and Abhinav Gupta. Unsupervised learning of visual representations using videos. In *Proceedings of the IEEE international conference on computer vision*, pages 2794–2802, 2015. 2
- [25] Xiaolong Wang, Kaiming He, and Abhinav Gupta. Transitive invariance for self-supervised visual representation learning. In *Proceedings of the IEEE international conference on computer vision*, pages 1329–1338, 2017. 2



- [26] Lin Yen-Chen, Andy Zeng, Shuran Song, Phillip Isola, and Tsung-Yi Lin. Learning to see before learning to act: Visual pre-training for manipulation. In *2020 IEEE International Conference on Robotics and Automation (ICRA)*, pages 7286–7293. IEEE, 2020. 2
- [27] Asano YM., Rupprecht C., and Vedaldi A. A critical analysis of self-supervision, or what we can learn from a single image. In *International Conference on Learning Representations*, 2020. 2
- [28] Richard Zhang, Phillip Isola, and Alexei A Efros. Colorful image colorization. In *European conference on computer vision*, pages 649–666. Springer, 2016. 2
- [29] Richard Zhang, Phillip Isola, and Alexei A Efros. Split-brain autoencoders: Unsupervised learning by cross-channel prediction. In *Proceedings of the IEEE Conference on Computer Vision and Pattern Recognition*, pages 1058–1067, 2017. 2
- [30] Richard Zhang, Phillip Isola, Alexei A Efros, Eli Shechtman, and Oliver Wang. The unreasonable effectiveness of deep features as a perceptual metric. In *Proceedings of the IEEE conference on computer vision and pattern recognition*, pages 586–595, 2018. 2, 6